Title

Evaluating uncertainty in Landsat-derived postfire recovery metrics due to terrain, soil, and shrub type variations in southern California

Journal

GIScience & Remote Sensing, 57(3)

ISSN

1548-1603

Authors

Storey, Emanuel A
Stow, Douglas A
Roberts, Dar A

Publication Date

2020-04-02

DOI

10.1080/15481603.2019.1703287

Peer reviewed

Published in final edited form as:
GIsci Remote Sens. 2020 ; n/a: . doi:10.1080/15481603.2019.1703287.

Evaluating uncertainty in Landsat-derived postfire recovery metrics due to terrain, soil, and shrub type variations in southern California

Emanuel A. Storey[a], **Douglas A. Stow**[a], **Dar A. Roberts**[b]

[a]Department of Geography, San Diego State University, San Diego, CA, USA;

[b]Department of Geography, University of California-Santa Barbara, Santa Barbara, CA, USA

Abstract

Temporal trajectories of apparent vegetation abundance based on the multi-decadal Landsat image series provide valuable information on the postfire recovery of chaparral shrublands, which tend to mature within one decade. Signals of change in fractional shrub cover (FSC) extracted from time-sequential Normalized Difference Vegetation Index (NDVI) data can be systematically biased due to spatial variation in shrub type, soil substrate, or illumination differences associated with topography. We evaluate the effects of these variables in Landsat-derived metrics of FSC and postfire recovery, based upon three chaparral sites in southern California which contain shrub community ecotones, complex terrain, and soil variations. Detailed validations of prefire and postfire FSC are based on high spatial resolution ortho-imagery; cross-stratified random sampling is used for variable control. We find that differences in the composition and structure of shrubs (inferred from ortho-imagery) can substantially influence FSC-NDVI relations and impact recovery metrics. Differences in soil type have a moderate effect on the FSC-NDVI relation in one of the study sites, while no substantial effects were observed due to variation of terrain illumination among the study sites. Arithmetic difference recovery metrics – based on NDVI values that were not normalized with unburned control plots – correlate in a moderate but significant manner with a change in FSC (R^2 values range 0.47–0.59 at two sites). Similar regression coefficients resulted from using Landsat visible reflectance data alone. The lowest correlations to FSC resulted from Soil-Adjusted Vegetation Index (SAVI) and are attributed to the effects of the soil-adjustment factor in sparsely vegetated areas. The Normalized Burn Ratio and Normalized Burn Ratio 2 showed a moderate correlation to FSC. This study confirms the utility of Landsat NDVI data for postfire recovery evaluation and implies a need for stratified analysis of postfire recovery in some chaparral landscapes.

Keywords

Postfire recovery; soil background effects; biomass; topographic illumination; signal-to-noise ratio

CONTACT Emanuel A. Storey, estorey@sdsu.edu.

Disclosure statement
No potential conflict of interest was reported by the authors.

Introduction

Ecological context

The recovery of natural vegetation from fire disturbance is a key element of ecological resilience, which can determine landscape response to environmental change over long time periods (Turner 2010). Failure of plant communities to reestablish in structure and composition after a fire may cause undesirable ecological changes and may even alter future patterns of fire risk and severity (Keeley and Brennan 2012). Diminished postfire recovery has been observed in regions subject to abnormally frequent or severe fire, relative to the historical fire regimes in which native plants evolved (Zedler, Gautier, and McMaster 1983; Bond and Keeley 2005). Invasion of exotic plants or mortality of native seedlings due to drought following a fire can also degrade vegetated landscapes (Pratt et al. 2014; Venturas et al. 2016). Spatial patterns and rates of postfire recovery are influenced by micro-climatic and edaphic conditions and vary substantially among plant species (Keeley and Davis 2007).

Evergreen sclerophyll shrub communities (chaparral) of southern California comprise biologically diverse, human-impacted, and naturally fire-prone vegetation province. Hazardous behavior and ecological impacts of fire in this region have been linked to anthropogenic ignitions, climatic change, and propagation of invasive plant species (Syphard et al. 2007). Management of fire hazard and ecological change in chaparral might be improved by understanding past vegetation dynamics and, ideally, anticipating fire-vegetation feedbacks under projected climate and fire regime scenarios (Batllori et al. 2019).

Remote sensing of postfire recovery

Given the variety of potential controls on vegetation development, assessment of shrub recovery among diverse sites having variable fire history, climatic, and ecological characteristics may provide a uniquely systematic understanding of postfire recovery in the chaparral bioregion. Satellite remote sensing has great utility for characterizing large-scale spatial patterns and temporal changes of Mediterranean-type shrub vegetation (Shoshany 2000; Gitas et al. 2012). Monitoring vegetation recovery entails multi-temporal estimates of plant abundance, typically in units of aboveground biomass or projective canopy cover (Stow 1995; Peterson and Stow 2003). The Landsat (4, 5, 7, and 8) image archive was collected at nominal 16-day intervals over the period of 1984 to present, offering a long-term and consistent record of surface dynamics which is widely used to study fire-related phenomena (Shoshany 2000). Spectral vegetation indices (SVIs) including Normalized Difference Vegetation Index (NDVI) and Normalized Burn Ratio 2 (NBR2) have been deemed most sensitive to change in semi-arid shrub vegetation (Vila and Barbosa 2010; Chen et al. 2011; Meng et al. 2014). Landsat surface reflectance (SR) imagery recently offered by the United States Geologic Survey (USGS) reduces artifacts of atmospheric and solar irradiance variations, thus enhancing signals of vegetation change (Masek et al. 2006). Valuable short-wave infrared wavebands (~1.−55–1.75 μm and ~2.09–2.35 μm) covered by Landsat sensors are not captured by contemporaneous satellite missions (*e.g.* Advanced Very High-Resolution Radiometer) nor by color-infrared (CIR) aerial frame ortho-imagery. The 30 m spatial resolution of Landsat imagery is adequate for monitoring shrublands, which can be highly heterogeneous (Masek et al. 2013). Archived CIR ortho-imagery typically

provides a spatial resolution of 0.3 to 1.0 m, albeit with inconsistent seasonal timing and variable image quality (Wing, Burnett, and Sessions 2014). A robust technique of tracking vegetation change is to leverage the temporal qualities of the Landsat record, employing CIR ortho-imagery for sensitivity assessment (Fraser et al. 2011).

Pixel tracking based on anniversary-date image series may aid in reducing artifacts stemming from sun orientation, growth phenology, and surface moisture variations (Stow 1995; Hope, Tague, and Clark 2007; Ju and Masek 2016). Declines in multi-annual Landsat SVI trajectories (i.e. pixel-based temporal trends) are shown to correlate with reduced shrub cover resulting from limited recovery (Storey, Stow, and O'Leary 2016). The arithmetic difference and ratio metrics have been used to contrast prefire *versus* postfire SVI trajectories associated with recovery (Díaz-Delgado, Salvador, and Pons 1998):

$$\text{Difference Recovery Metric} = \text{SVI}_{\text{postfire}} - \text{SVI}_{\text{prefire}} \quad (1)$$

$$\text{Ratio Recovery Metric} = \frac{\text{SVI}_{\text{postfire}}}{\text{SVI}_{\text{prefire}}} \quad (2)$$

where $SVI_{prefire}$ is the SVI trajectory value associated with mature vegetation in years preceding fire, and $SVI_{postfire}$ is the SVI trajectory value at the expected time of full potential recovery. Trajectories can be characterized using multi-annual means, medians, or best-fit regression functions (linear, logarithmic, or piece-wise) (Röder et al. 2008). Metrics which also incorporate a postfire SVI data point that precedes shrub recovery (SVI_{burned}) may aid to normalize for vegetation abundance and soil background variability (Storey, Stow, and O'Leary 2016).

$$\text{Scaled Recovery Metric} = \frac{\text{SVI}_{\text{postfire}} - \text{SVI}_{\text{burned}}}{\text{SVI}_{\text{prefire}} - \text{SVI}_{\text{burned}}} \quad (3)$$

Problem statement

Further research is needed to evaluate the accuracy of Landsat-based metrics of postfire recovery when applied in a spatially explicit manner for analysis of large areas. We evaluate the correlations of several Landsat-based SVIs and derived recovery metrics with respect to fractional shrub cover (FSC) and fire-driven change in FSC (hereafter: *dFSC*) in heterogeneous chaparral. The major emphasis of this study is to evaluate biases introduced by shrub biomass, soil, and terrain variations, which may invalidate statistical analyses of Landsat-based postfire recovery data within or amongst sites (*cf.* Henry and Yool 2002).

The NDVI is primarily sensitive to plant cover in a wide range of arid and semi-arid environments (Montandon and Small 2008). Biomass and leaf area index (LAI) also correlate with NDVI (r= 0.84–0.95) from samples of eight prevalent chaparral species (Gamon et al. 1995). Variations in foliar pigment content, light use efficiency, canopy structure, and non-photosynthetic materials including leaf litter can also contribute to

variations in NDVI (Yang and Guo 2014). Variations in shrub biomass are a major source of uncertainty in remotely sensed estimates of chaparral cover (*cf.* Peterson and Stow 2003).

Variations of soil reflectance (brightness) and hue (color) also may add uncertainty to FSC estimations. Soils of high visible reflectance tend to lower NDVI values in arid rangelands, when the factor of plant cover is controlled (Huete and Jackson 1987). Analytical models suggest that low-reflectance soils cause nonlinearity in the relation of NDVI to FSC. Soil moisture may also influence reflectance (Todd and Hoffer 1998); water-holding capacity and drainage rates can vary spatially within and amongst soil types (Farrar, Nicholson, and Lare 1994). Chrono-sequence analysis suggests that soils may be a significant source of spectral reflectance variation in chaparral landscapes (Peterson and Stow 2003). Previous work has not evaluated the effects of soil variation on postfire chaparral recovery trajectories that are based on pixel tracking.

Illumination variability may also contribute to error in change detections which are based on multi-temporal satellite imagery (Song and Woodcock 2003). Landsat SR images provided by USGS correct for atmospheric scattering, but are subject to Lambertian reflectance variation due to terrain (Masek et al. 2006). Backscatter due to non-Lambertian reflectance may contribute to error in chaparral abundance estimates (Roberts, Smith, and Adams 1993), although scattering effects are similar in red and NIR wavelengths and thus potentially normalized by the NDVI formula (Lee and Kaufman 1986). Terrain can also affect illumination through shading, which increases the ratio of diffuse-to-direct surface irradiance (Giles 2001). This effect is pronounced in short visible wavelengths most prone to atmospheric scattering (Liu and Yamazaki 2012). Previous research has not resolved the signal-to-noise ratio for remote sensing of postfire shrub recovery in relation to terrain variability. A clearer understanding of the potential error sources emphasized above may clarify whether data normalization or geographic sample stratification is required for a large-scale study of postfire chaparral recovery based on Landsat SR image series.

Research objectives

The primary objective of this study is to assess the sensitivity and accuracy of metrics derived from Landsat SVI trajectories for monitoring postfire chaparral recovery. This study focuses on potential systematic biases in SVI trajectories due to soil, vegetation, and terrain differences. We evaluate three burned study sites of 90–140 $km^{2,}$ which each contains lowland-to-montane chaparral transitions typical of southern California. These study sites also exhibit internal variations in postfire shrub recovery, as determined from high spatial resolution ortho-imagery. Based upon correlative empirical analysis of these sites, this research addresses the following questions:

1. How sensitive are Landsat-derived SVIs to spatial and temporal variations in fractional shrub cover?
2. How do variations among terrain, soil, and shrub biomass strata affect the sensitivity of SVI trajectories to shrub cover change due to limited recovery?

3. Which recovery metrics, landscape stratifications, or time-series normalization procedures are most appropriate in the large-scale assessment of chaparral recovery?

Methods

Analytical framework

Figure 1 illustrates the data processing and analysis framework used in this study. We employed high spatial resolution, multi-temporal ortho-imagery to classify soil and shrub types, and to derive gridded validations of FSC and of fire-induced dFSC. Digital terrain data were used to map spatial variation of solar illumination in Landsat scenes acquired on or near June solstice, over the period 1984–2018. The SVIs selected for this study collectively involve each of the visible, near-infrared, and shortwave-infrared wavebands sampled by Landsat sensors. Phenological normalization and several trajectory-based recovery metrics applied in previous studies were evaluated. Statistical relations of dFSC to Landsat SVI recovery metric data are compared amongst soil, vegetation, and illumination classes based upon a cross-stratified sampling and variable-control approach. Methodological steps are described in greater detail in the following sections.

Data sets and preprocessing

Detailed maps of prefire land cover were based upon 1 m digital CIR ortho-image quarter-quads captured between 1996 and 2002 and provided by USGS (earthexplorer.usgs.gov). The postfire image set is composed of four-band (red, green, blue, and near-infrared) images of 0.6 m spatial resolution, captured by the National Agricultural Imagery Program (NAIP) in 2016. The ortho-image sets were resampled to consistent spatial resolutions of 1 m and radiometrically normalized by histogram matching the prefire images (i.e. forcing value-frequency bin functions to match) in reference to the 2016 images of corresponding frame locations. Green, red, and near-infrared spectral bands were normalized separately. We derived spectral transforms from the ortho-images including NDVI, average intensity in red and green bands (I_{RG}), and a normalized ratio index which contrasts red *versus* green band values ($I_{R/G}$). These spectral transforms supported classification of shrub cover, shrub type, and soil type.

Landsat data used in this study comprise a 34-year (1984–2018) image series which were processed to directional SR through the Land Surface Reflectance Climate Data Record (LSRCDR) (espa.cr.usgs.gov) (Masek et al. 2006; Vermote et al. 2016). Landsat 4–5 (Thematic Mapper) data cover the period of 1984–2011, and Landsat 8 (Operational Land Imager) data cover the period 2013–2018 (in path-rows 40–37 and 41–36). Quality assurance maps provided by LSRCDR and based on the *Fmask* algorithm (Zhu and Woodcock 2012) were used to preclude image pixels containing cloud or cloud-shadow in the study areas. Landsat SVI images used in postfire recovery assessment were resampled to 3-X-3 pixel blocks (90 m spatial resolution) to reduce artifacts of geometric misregistration with respect to the ortho-imagery (*cf.* Hope, Tague, and Clark 2007). These Landsat images were selected annually near June solstice (10 June to 14 July), associated with maximal solar illumination, high shrub growth, and senescence in regional under-storey herbs. Potentially

useful SVIs including NDVI (Rouse et al. 1974), NBR (Key and Benson 1999), NBR2 (Key and Benson 2006), Soil-Adjusted Vegetation Index (SAVI) (Huete 1988), and visible band (red, green, and blue) mean reflectance (R_{vis}) were used to generate separate pixel trajectories. Custom maps of burned areas were generated from 30 m spatial resolution NBR images acquired in various seasons.

Study area selection

We selected study areas following a preliminary analysis of fire history, plant distribution, and postfire recovery patterns across southern California (Figure 2). All areas that burned within the study period (1984–2018) and were also classified as *chamise* chaparral according to CALVEG community type maps (www.fs.usda.gov) were preliminarily selected. Historical fire perimeters were acquired from California Fire Resource and Protection (FRAP) (frap.cdf.ca.gov). Fire perimeter dates were used to identify areas containing mature vegetation in both early and late phases of the study period, based on the general 10-year recovery time of chamise chaparral (Henry and Hope 1998; Hope, Tague, and Clark 2007). We excluded sites that burned since 2007 or in designated prefire years (1980–1995). We visually compared prefire *versus* postfire ortho-images to identify sites having internal variation in postfire recovery. Additional site criteria included: 1) salient variation in soil type; 2) complex topography; 3) presence of montane chaparral (associated with high biomass); and 4) sage scrub in low-elevation portions of the same fire perimeters, which contained mainly chamise. We selected three study sites (among five that met the above criteria) that showed the greatest variations in the soil, shrub, and terrain characteristics of interest. Figure 2 illustrates the terrain and vegetation abundance patterns of the selected study sites.

Due to potential errors in the fire perimeter data (*cf.* Syphard and Keeley 2017), we produced custom maps of fire history since 1984 at each study site. The custom burned extent maps were constructed by applying exceedance thresholds to the Relative Delta NBR (RdNBR) index (Miller and Thode 2007):

$$\mathrm{RdNBR} = \frac{\mathrm{NBR}_{\mathrm{prefire}} - \mathrm{NBR}_{\mathrm{postfire}}}{\sqrt{\mathrm{NBR}_{\mathrm{prefire}}}} \quad (4)$$

The RdNBR is sensitive to relative variations in burn severity among admixed vegetation types (Miller and Thode 2007). The total burned area and number of unique fire histories (i.e. years of the study period in which fire occurred) are as follows: Site A – 140 km^2 (five histories); Site B – 90 km^2 (four histories); and Site C – 110 km^2 (two histories).

Phenological control

Control sites composed of unburned chamise were selected by closest proximity (within 5 km of each study site) in order to normalize for inter-annual variations in growth phenology and moisture condition in the Landsat SVI series. Rather than a simple quotient of the annual SVI values in burned *versus* control sites (Díaz-Delgado, Salvador, and Pons 1998), our phenological normalization quantified the magnitude of deviation (SVI_{var}) in annual SVI values ($cSVI_{annual}$) at each control site with respect to its own long-term trajectory

($cSVI_{mean}$), computed as the mean of 10 years which comprise the prefire and postfire phases:

$$\mathrm{SVI}_{\mathrm{var}} = \frac{\mathrm{cSVI}_{\mathrm{annual}}}{\mathrm{cSVI}_{\mathrm{mean}}} \quad (5)$$

Per-pixel SVI values associated with burned areas ($bSVI_{annual}$) were thereby adjusted to yield the normalized values ($nSVI_{annual}$):

$$\mathrm{nSVI}_{\mathrm{annual}} = \mathrm{bSVI}_{\mathrm{annual}} - \mathrm{bSVI}_{\mathrm{annual}} * \left(\mathrm{SVI}_{\mathrm{var}} - 1\right) \quad (6)$$

Landsat SVI trajectories and metrics

Mean SVI values of 5 years preceding the initial fire at each study site were used to represent prefire trajectories ($SVI_{prefire}$), which are relatively stable through time. Postfire trajectories were derived from linear best-fit (ordinary least-squares) regression functions over the period 2014–2018, which exhibits vegetation increase at sites that burned after 2004. The $SVI_{postfire}$ values were based on the termini of these linear trajectories at the time point of 21 June 2016, consistent with the postfire ortho-imagery used in validation. The SVI_{burned} trajectory points were based on SVI values from summer following the most recent fire in any location within the study areas. Trajectories were derived in separate workflows that involved or omitted (for comparative evaluation) phenological normalization based on unburned control sites. Finally, we applied several metrics of change between the prefire and postfire trajectories (Equations (1–3)).

Vegetation classification

Chaparral described herein as *sub-montane* consists mainly of chamise, a community dominated by *Adenostoma fasciculatum* and often admixed with *Ceanothus spp.* and other species found in adjacent communities (*cf.* Sawyer, Keeler-Wolf, and Evens 1995). Montane chaparral is highly diverse but typified by *Arctostaphylos spp.*, *Cercocarpus spp.*, *Quercus agrifolia*, and *Rhus ovata*. Montane parts of our study sites contain sparsely admixed *Cupressus forbesii* (Site A), *Quercus agrifolia* (Site B), and *Pinus coulteri* (Site C). Sub-shrubs described herein consist of sage scrub, typified by *Salvia spp.*, *Eriogonum spp.*, *Baccharis spp.*, and *Artemisia californica* (Schoenherr 1992). Prevalent species were inferred from the CALVEG maps but not mapped explicitly, due to the 1-m spatial resolution and broad spectral wavebands of the ortho-imagery. Custom, image-derived vegetation classes were used to infer relative differences in shrub size and composition at each site, which may affect recovery metrics based on Landsat SVIs. Strong contrasts in NDVI based on ortho-imagery were used as rudimentary proxies of biomass variation (*cf.* Cho et al. 2007).

High spatial resolution shrub cover maps based on NDVI, I_{RG}, and $I_{R/G}$ were constructed in ERDAS Imagine® using a multi-criterion, decision-tree classification. Vegetation classes included: *herbaceous* (predominantly senesced grass) and shrub types including *sub-shrub* dominated, *sub-montane* chaparral, and montane chaparral (mainly obligate re-sprouting shrubs in mesic locations). Ground-based observations of shrub type distribution were recorded at Site A in order to facilitate ortho-image classification. Inferences of shrub types

made for Site A were extended to Site B and Site C, based on careful visual interpretation of ortho-imagery and supplemented by CALVEG maps. Exceedance thresholds applied to the spectral transforms were identified by pixel query, and adjusted by 10–25 iterative classification trials per frame. This approach was used by Storey, Stow, and O'Leary (2016) based on similar data sets and landscapes, yielding overall classification accuracy of 85–95%. The shrub classification maps were used to estimate type-specific as well as aggregated (i.e. shrub *versus* non-shrub) fractional cover within 90-m grid elements aligned to Landsat pixel edges (Figure 3).

Soil and terrain classification

Soil type maps were based on a reclassification of pixels associated with no vegetation (i.e. soil and rock exposures) in the shrub type maps. Multiple threshold criteria were applied to the I_{RG} and $I_{R/G}$ transforms in order to discriminate soil types using a decision tree. Soils in each study area were classified as *albic* (high-reflectance), *argillic* (red hue), or *indistinct* (mix or intermediate of albic and argillic). Soil maps were derived from the 2016 ortho-imagery, which showed higher soil exposure and minimal leaf litter accumulation as compared to the prefire imagery. Kernel-based focal operators were used to aggregate soil features based on class majority and contiguity. Soil map pixels in zones of dense shrub cover were assigned to a null class.

Variations in topographic illumination were estimated from sun-sensor-terrain orientation geometries. We derived Cos(*i*) using the formula provided by Ediriweera et al. (2013), from a 10 m digital elevation model (nationalmap.gov). Zeniths and azimuths were based on nominal June-solstice parameters, consistent with the Landsat image series. Cos(*i*) data sets were classified into three ordinal strata (<0.8, 0.8–0.9, and >0.9), which are approximate data quantiles of each study site. Figure 4 shows examples of the shrub type, illumination, and soil type maps which we tabulated to 90-m grids along with the FSC estimates.

Statistical sampling

Our approach required shrub, soil, and illumination class dominance to be determined for each 90-m grid element, in order to cross-stratify among these landscape variables for the purpose of factor control. Criteria for predominance were as follows: shrub class: >60 percent, soil class: >80 percent, and illumination class: >70 percent. Grid elements not dominated by any single class among the variables were excluded from the analysis, which substantially limited the number of possible sample locations. Cross-stratification followed these selection rules: samples used to evaluate variation in shrub type were constrained to high-illumination and indistinct soil classes; soil type analysis samples were constrained to sub-montane chaparral and high-illumination classes; illumination analysis samples were constrained to sub-montane chaparral and indistinct soil zones.

These cross-strata helped isolate the potential effect of each variable upon the sensitivity of Landsat SVI trajectories to FSC and dFSC. Random points were generated in order to distribute sample locations within the gridded zones conforming to the cross-stratification criteria. The random samples consisted of 30 to 60 points per stratum, generated in equal number among the strata of each variable within each study site. A total of 326 to 378 points

per study site remained once spurious points associated with human-caused land transformation had been eliminated. Resultant tabular data were analyzed visually using X-Y data plots and by multivariate linear regressions conducted in MS Excel®, based on 95% confidence levels.

Results

Relations of Landsat SVIs to shrub cover variation

Relations between Landsat SVIs and FSC (mapped primarily based on NDVI from aerial imagery) were evaluated using linear regression tests based upon goodness-of-fit (R^2), line intercepts, and slope coefficients. The Landsat SVIs evaluated in this study (NDVI, SAVI, NBR, NBR2, and R_{vis}) are significantly correlated with FSC at each study site. Figure 5 contrasts R^2 values associated with these regressions, which relate prefire and postfire FSC to Landsat SVI trajectory values that are raw (unnormalized), and those that were normalized using unburned control plots. R^2 values generally range from 0.5 to 0.7 in the prefire data sets, and 0.60 to 0.85 in the postfire data sets. Higher correlation of the postfire samples is attributable to greater accuracy of the postfire shrub cover maps, which are based on higher quality imagery. In all samples, Landsat NDVI exhibited the strongest covariation with FSC among the SVIs. NBR and R_{vis} indices yielded similar R^2 values, having a greater correlation to FSC than NBR2 and SAVI. R^2 values were notably similar in normalized and unnormalized samples. Normalized samples were lower in R^2 (by 0.02) based on aggregate means of all samples derived from NDVI.

Results presented hereafter pertain to Landsat NDVI, because this SVI exhibited the highest sensitivity to FSC and is, therefore, most practically applicable. Best-fit linear functions based on the postfire FSC and NDVI trajectory data sets are organized according to cross-stratified sample groups and represented in Figure 6. Corresponding p-values, from multi-variate linear regressions used to evaluate the variables (in conjunction with FSC) as explanatory factors of Landsat NDVI, are provided in Table 1. Shrub type had a significant influence on NDVI, once the explanatory power of FSC was accounted for in the multivariate regression tests. The montane chaparral samples exhibited a statistically significant yet moderate influence on the NDVI-FSC relations in Site A and Site B, based on regression slope and intercept differences (Figure 6). Illumination variability led to significant variability in NDVI at Site B (Table 1), but less so at Site A and Site C. One or more soil strata were significant factors at each study site (Table 1). The sample from the argillic soil stratum at Site B showed a distinct slope and intercept, as compared to the aggregated data shown by transparent circles (Figure 6).

The varying landscape factors defining the stratum memberships appear to explain a substantial portion of the variability observed in the FSC-NDVI regressions. Shrub type is evidently the most substantial contributor to this variance at Site A and Site B, while the effect of soil type is most evident at Site C. The cross-stratified samples, however, do not provide absolute control of admixture effects among the soil, vegetation, and terrain factors. For example, the low-illumination sample from Site A is associated with relatively high FSC (and therefore biomass, due to mesic terrain positioning) even though it is primarily covered by sub-montane chaparral. The aggregate-level correlation of NDVI to FSC (R^2 values range

from 0.72 to 0.87) implies potential sensitivity to temporal changes in shrub cover, despite the effects of land cover and terrain.

Evaluation of Landsat NDVI-based recovery metrics

Postfire recovery estimates derived from Landsat NDVI trajectories exhibited statistically significant relations to dFSC based on difference, ratio, and scaled recovery metrics, calculated with and without control-plot normalization. R^2 values of univariate linear regressions comparing Landsat NDVI recovery metric data to dFSC were in the range of 0.3 to 0.6 among the study sites and recovery metric variants (Table 2). Differences in the dFSC-NDVI relations among the study sites (Table 2) tend to reflect those observed among the FSC-NDVI relations (Table 1), where Site B exhibited the greatest unexplained variance. Examining mean values from all study sites, dFSC explains 44% to 47% of the variance in difference metric and ratio metric data, but only 15% to 18% in the scaled recovery metric data. The difference and ratio metrics exhibit similar and relatively high mean R^2 values based on the unnormalized samples (0.47). The difference recovery metric is selected for subsequent analyses of vegetation trajectories with respect to landscape variations. Raster maps illustrating results from the difference recovery metric based on Landsat NDVI are provided in Figure 7.

Evaluation of landscape influences on NDVI-based recovery metrics

Scatterplots illustrating the relation of dFSC to Landsat NDVI difference metric data according to stratified samples are provided in Figure 8. Differences among best-fit line slopes and intercepts (according to strata) follow similar patterns in dFSC as in FSC (Figure 6). The most substantial effects on dFSC are associated with shrub type, and these are most pronounced at Site A in the montane shrub class. As compared to the FSC-NDVI trends in Figure 6, a greater distinction is observed with respect to the sub-shrub-dominated class in all study sites (Figure 8). The dFSC trend lines of montane *versus* sub-montane shrub types are less distinct at Site B and Site C (comparing Figures 6 and 8) than Site A. Trend lines do not differ consistently or substantially among illumination classes (Figure 8). Effects of soil type on Landsat NDVI difference metric values appear greatest in Site B, but are insubstantial in Site A and Site C.

The significance (p-values) of variability in the Landsat NDVI difference metrics due to stratum membership is shown in Table 3. Landsat NDVI difference metrics exhibited significant variation in each of the variables and strata for Site B, except for the albic soil stratum. Site A exhibits a significant difference only for the montane chaparral stratum; albic soil, low-illumination, and sub-shrub-dominated strata are significant at Site C. Some of the variables that are significant based on Table 3 are deemed insubstantial in magnitude based on relative differences among regression slopes (Figure 8).

Discussion and conclusions

Results from this study clarify our understanding of uncertainty in Landsat-based postfire recovery metrics when applied to intermixed chaparral types over complex landscapes. This study has addressed the following objectives: (1) to evaluate the sensitivity of key Landsat

SVIs to spatial and temporal variations of FSC; (2) to assess the relative importance of terrain, soils, and shrub biomass as causes of variation in postfire recovery metrics based on NDVI; and (3) to reevaluate the utility of control-plot normalization and arithmetical metrics for chaparral recovery assessment. We foresee potential advantages in stratifying by the landscape variables examined, in order to improve assessment postfire recovery in heterogeneous chaparral based on Landsat SVI series.

Our results corroborate previous studies which indicate that NDVI is a uniquely accurate indicator of FSC in Mediterranean-type shrublands (Baret and Guyot 1991; Clemente, Navarro-Cerrillo, and Gitas 2009; Vila and Barbosa 2010; Calvão and Palmeirim 2011). Based on a substantial number and diversity of sample locations, we find that NBR is more sensitive than NBR2 to variations in FSC. This finding does not necessarily contradict previous findings that NBR2 is the most sensitive SVI to late-stage, gradual changes in shrub abundance (Carreiras, Pereira, and Pereira 2006; Storey, Stow, and O'Leary 2016). Results of the present study suggest that visible reflectance (R_{vis}) variations are more correlated to FSC in chaparral than several commonly used SVIs. This finding suggests that signals of diminished recovery in chaparral stem not only from a decline in plant (photo-synthetically active) reflectance, but from soil exposure as well. A similar result was reported by Franklin, Davis, and Lefebvre (1991) for an Oak woodland in California. In semi-arid landscapes with bright soil types, the predominant influence on NDVI is shrub cover rather than biomass or LAI (Calvão and Palmeirim 2011). The typically low stature and low LAI of shrublands may explain why SAVI was least correlated to FSC in this study, a result which we attribute to the non-linear effect of the soil-adjustment factor (Huete 1988). Changes in soil exposure detectable by NDVI are most relevant to soil erosion, evaporation, and climatic forcing dynamics in chaparral environments (Pase and Lindenmuth 1971; Anderson and Goulden 2011).

By means of cross-stratified sampling, we assessed the sensitivity of SVIs and of SVI-based recovery metrics to soil, shrub, and illumination factors. The variables selected in this study appear to explain the greater portion of the observed variance in the FSC-NDVI regression samples. We find that montane shrubs associated with relatively high infrared reflectance can exhibit NDVI-FSC relations that differ moderately from those of sub-montane shrubs. At sites with similar characteristics as Otay Mountain (Study Site A), where montane chaparral is admixed with small cypress trees, stratification using detailed shrub community maps would reduce uncertainty regarding FSC-SVI relations.

Differences in soil type can also influence NDVI-FSC relations, though moderately, based on the results of this study. Effects of terrain illumination variability on NDVI-FSC relations appear negligible. This finding is presented with some uncertainty; however, as shrub cover maps derived from ortho-images are taken to be less accurate in low-illumination areas subject to shading. More importantly, our findings regarding terrain illumination are based on summer-solstice Landsat data and should not be extended to other seasons during which terrain shading is more prevalent.

A unique aspect of this study is its focus on vegetation change associated with postfire recovery, whereas many other studies have assessed the sensitivity of remotely sensed

images to static vegetation patterns (e.g. Carlson and Ripley 1997; Xiao and Moody 2005). A major insight was that landscape factors that significantly affect FSC-SVI relations are likely to accentuate uncertainty in postfire recovery metrics derived from SVI trajectories. This is especially true for differential sensitivity to shrub types, including montane and sub-shrub dominated shrublands which typically adjoin chamise chaparral along eco-climatic gradients. The sensitivity of NDVI to change in the cover is especially low for low-elevation shrub communities (*i.e.* sage scrub) that we examined, which implies that regional studies of postfire recovery may benefit from stratification according to shrub types. The slow recovery of *C. forbesii* (~40 years) at Otay Mountain may explain why this site showed the strongest influence of montane chaparral in its dFSC-NDVI relation (de Gouvenain and Ansary 2006). Differences in soil type may only warrant stratified sampling where soil hues and associated spectral reflectances are highly varied, such as Volcan Mountains (Study Site B). The choice to stratify Landsat-based recovery metric data should also depend upon how the results are to be utilized.

The accuracy of Landsat-based recovery metrics as spatially explicit representations of dFSC in chaparral is moderate, based on the R^2 values (0.43–0.59) obtained in this study for the sites with higher-confidence FSC validation estimates. We attribute the low average R^2 value (0.3) for Site B to an exceptional diversity of shrub species occurring there, due to differential effects of canopy structure and pigmentation on SVI values (Yang and Guo 2014). Mapping highly degraded, moderately degraded, and well-recovered zones appears tractable based on the correlations of Landsat NDVI to dFSC. Categorical maps of recovery levels may facilitate the selection of sites for more detailed examination using high spatial resolution imagery or ground-based observation.

Low performance of the scaled recovery metric relative to difference and ratio metrics appears to contradict Storey, Stow, and O'Leary (2016). Key differences in the application of scaled recovery metric in the latter study include: (1) terrain, shrub type, and soils were generally uniform, and (2) samples were mostly collected within a single fire history zone. We attribute the low performance of the scaled recovery metric to variations in burned surface conditions among the SVI images from different postfire years; this is evinced by the higher performance of this metric at the study site that contained only two fire histories. Our reasoning is consistent with Veraverbeke et al. (2010), who show that rapid changes in surface reflectance (owing to translocation of charred pyric residuals and development of early-successive plants) lead to a substantial intra-seasonal change of SVI values. Hence, the scaled recovery metric may be unsuitable for application in areas that contain varied fire histories during a study period.

The minor difference in accuracy of postfire recovery assessments that involved phenological normalization (compared to unnormalized) is a surprising outcome of this study, as such normalizations are shown to reduce the correlation of NDVI with respect to annual precipitation by 0.26 to 0.58 (Storey, Stow, and O'Leary 2016). While reducing data scatter, normalization did not substantially affect the slopes or intercepts of the trajectories, derived from best-fit linear functions. It is possible that utility of normalization would be enhanced by pixel-specific control site associations, as proposed by Lhermitte et al. (2011). Nonetheless, our results suggest that effects of surface condition variations are sufficiently

reduced by selection of anniversary-date (summer solstice) images and computation of best-fit trajectories, as to produce useful estimates of postfire recovery in chaparral.

This study highlights the utility of Landsat SVI trajectories for postfire recovery assessment, being more replicable and efficient than shrub cover mapping based upon high spatial resolution, multi-temporal ortho-imagery. Our validations of shrub cover change required ~20 min per km^2 to produce, resulting in 90 person-hours to complete 300 km^2 of study areas. Region-wide postfire recovery assessment using ortho-imagery would thus be inefficient or intractable, relative to a Landsat-based approach. Techniques of postfire recovery assessment that are developed using Landsat data may later be applied to satellite image data of higher spatial resolution (including Sentinel-2), which constitute ever-growing data archives. Improved technology for assessment of postfire recovery may increase the efficacy of conservation practices including restoration.

This study represents a contribution to the broad literature on the use of satellite remote sensing to resolve land cover changes at sub-pixel scales, and attendant questions of sensitivity and signal-to-noise ratio. Specifically, we demonstrate that shrub biomass variability in chaparral may elicit redesign of analytical techniques used to evaluate postfire recovery based on remotely sensed imagery. The analytical framework employed in this study is potentially applicable to other bioregions and change detection problems.

Funding

This research was supported primarily by an Earth & Space Science Fellowship [training grant # 80NSSC17K0393] awarded by the National Aeronautics & Space Administration (NASA). No conflicts of interest are reported.

References

Anderson RG, and Goulden ML. 2011 “Relationships between Climate, Vegetation, and Energy Exchange across a Montane Gradient.” Journal of Geophysical Research: Biogeosciences 116 (G01026): 1–16. doi:10.1029/2010JG001476.

Baret F, and Guyot G. 1991 “Potentials and Limits Of Vegetation Indices for LAI and APAR Assessment.” Remote Sensing of Environment 35 (2–3): 161–173.

Batllori E, De Cáceres M, Brotons L, Ackerly D, Moritz M, and Lloret F. 2019 “Compound Fire-drought Regimes Promote Ecosystem Transitions in Mediterranean Ecosystems.” Journal of Ecology 107 (3): 1187–1198. doi:10.1111/1365-2745.13115.

Bond WJ, and Keeley JE. 2005 “Fire as a Global ‘herbivore’: The Ecology and Evolution of Flammable Ecosystems.” Trends in Ecology and Evolution 20 (7): 387–394. doi:10.1016/j.tree.2005.04.025. [PubMed: 16701401]

Calvão T, and Palmeirim J. 2011 “A Comparative Evaluation of Spectral Vegetation Indices for the Estimation of Biophysical Characteristics of Mediterranean Semi-deciduous Shrub Communities.” International Journal of Remote Sensing 32 (8): 2275–2296. doi:10.1080/01431161003698245.

Carlson TN, and Ripley DA. 1997 “On the Relation between NDVI, Fractional Vegetation Cover, and Leaf Area Index.” Remote Sensing of Environment 62 (3): 241–252. doi:10.1016/S0034-4257(97)00104-1.

Carreiras JMB, Pereira JMC, and Pereira JS. 2006 “Estimation of Tree Canopy Cover in Evergreen Oak Woodlands Using Remote Sensing.” Forest Ecology and Management 223 (1): 45–53. doi:10.1016/j.foreco.2005.10.056.

Chen X, Vogelmann J, Rollins M, Ohlen D, and Key C. 2011 “Detecting Post-fire Burn Severity and Vegetation Recovery Using Multitemporal Remote Sensing Spectral Indices and Field-collected

Composite Burn Index Data in a Ponderosa Pine Forest." International Journal of Remote Sensing 32 (23): 7905–7927. doi:10.1080/01431161.2010.524678.

Cho MA, Skidmore A, Corsi F, Van Wieren SE, and Sobhan I. 2007 "Estimation of Green Grass/herb Biomass from Airborne Hyperspectral Imagery Using Spectral Indices and Partial Least Squares Regression." International Journal of Applied Earth Observation and Geoinformation 9 (4): 414–424. doi:10.1016/j.jag.2007.02.001.

Clemente R, Navarro-Cerrillo R, and Gitas I. 2009 "Monitoring Post-fire Regeneration in Mediterranean Ecosystems by Employing Multitemporal Satellite Imagery." International Journal of Wildland Fire 18 (6): 648–658. doi:10.1071/WF07076.

de Gouvenain RC, and Ansary AM. 2006 "Association between Fire Return Interval and Population Dynamics in Four California Populations of Tecate Cypress (Cupressus Forbesii)." The Southwestern Naturalist 51 (4): 447–455. doi:10.1894/0038-4909(2006)51[447:ABFRIA]2.0.CO;2.

Díaz-Delgado R, Salvador R, and Pons X. 1998 "Monitoring of Plant Community Regeneration after Fire by Remote Sensing" In Fire Management and Landscape Ecology, edited by Traboud L, 315–324. Fairfield, Washington: International Association of Wildland Fire.

Ediriweera S, Pathirana S, Danaher T, Nichols D, and Moffiet T. 2013 "Evaluation of Different Topographic Corrections for Landsat TM Data by Prediction of Foliage Projective Cover (FPC) in Topographically Complex Landscapes." Remote Sensing 5 (12): 6767–6789. doi:10.3390/rs5126767.

Farrar TJ, Nicholson SE, and Lare AR. 1994 "The Influence of Soil Type on the Relationships between NDVI, Rainfall, and Soil Moisture in Semiarid Botswana. II. NDVI Response to Soil Moisture." Remote Sensing of Environment 50 (2): 121–133. doi:10.1016/0034-4257(94)90039-6.

Franklin J, Davis FW, and Lefebvre P. 1991 "Thematic Mapper Analysis of Tree Cover in Semiarid Woodlands Using a Model of Canopy Shadowing." Remote Sensing of Environment 36 (3): 189–202. doi:10.1016/0034-4257(91)90056-C.

Fraser RH, Olthof I, Carrière M, Deschamps A, and Pouliot D. 2011 "Detecting Long-term Changes to Vegetation in Northern Canada Using the Landsat Satellite Image Archive." Environmental Research Letters 6 (4): 1–9. doi:10.1088/1748-9326/6/4/045502.

Gamon JA, Field CB, Goulden ML, Griffin KL, Hartley AE, Joel G, Penuelas J, and Valentini R. 1995 "Relationships between NDVI, Canopy Structure, and Photosynthesis in Three Californian Vegetation Types." Ecological Applications 5 (1): 28–41. doi:10.2307/1942049.

Giles PT 2001 "Remote Sensing and Cast Shadows in Mountainous Terrain." Photogrammetric Engineering and Remote Sensing 67 (7): 833–840.

Gitas I, Mitri G, Veraverbeke S, and Polychronaki A. 2012 "Advances in Remote Sensing of Post-fire Vegetation Recovery Monitoring-a Review" In Moisan T, Sathyendranath S, and Bouman H (Eds.) Remote Sensing of Biomass-Principles and Applications. (Open Access Publisher) Intech. doi:10.5772/20571.

Henry MC, and Hope AS. 1998 "Monitoring Post-burn Recovery of Chaparral Vegetation in Southern California Using Multi-temporal Satellite Data." International Journal of Remote Sensing 19 (16): 3097–3107. doi:10.1080/014311698214208.

Henry MC, and Yool SR. 2002 "Characterizing Fire-related Spatial Patterns in the Arizona Sky Islands Using Landsat TM Data." Photogrammetric Engineering and Remote Sensing 68 (10): 1011–1019.

Hope AS, Tague C, and Clark R. 2007 "Characterizing Post-fire Vegetation Recovery of California Chaparral Using TM/ETM+ Time-series Data." International Journal of Remote Sensing 28 (6): 1339–1354. doi:10.1080/01431160600908924.

Huete AR 1988 "A Soil-adjusted Vegetation Index (SAVI)." Remote Sensing of Environment 25 (3): 295–309. doi:10.1016/0034-4257(88)90106-X.

Huete AR, and Jackson RD. 1987 "Suitability of Spectral Indices for Evaluating Vegetation Characteristics on Arid Rangelands." Remote Sensing of Environment 23 (2): 213–232. doi:10.1016/0034-4257(87)90038-1.

Ju J, and Masek JG. 2016 "The Vegetation Greenness Trend in Canada and US Alaska from 1984–2012 Landsat Data." Remote Sensing of Environment 176: 1–16. doi:10.1016/j.rse.2016.01.001.

Keeley JE, and Davis FW. 2007 “Chaparral” In Terrestrial Vegetation of California, 3rd ed edited by Barbour MG, Keeler-Wolf T, and Schoenherr AA, 339–366. Berkeley: University of California Press.

Keeley JE, and Brennan TJ. 2012 “Fire-driven Alien Invasion in a Fire-adapted Ecosystem.” Oecologia 169 (4): 1043–1052. doi:10.1007/s00442-012-2253-8. [PubMed: 22286083]

Key CH, and Benson NC. 2006 “Landscape Assessment (LA)” In FIREMON: Fire Effects Monitoring and Inventory System. General Technical Report RMRS-GTR-164-CD, edited by Lutes DC, Keane RE, Caratti JF, Key CH, Benson NC, Sutherland S, and Gangi LJ, 1–55. Fort Collins, Colorado: US Department of Agriculture, Forest Service, Rocky Mountain Research Station.

Key CH, and Benson NC. 1999 “Measuring and Remote Sensing of Burn Severity.” Poster presented at the Joint Fire Science Conference and Workshop, Boise, Idaho, June 15–17. doi:10.1046/j.1469-1809.1999.6320101.x.

Lee TY, and Kaufman YJ. 1986 “Non-Lambertian Effects on Remote Sensing of Surface Reflectance and Vegetation Index.” IEEE Transactions on Geoscience and Remote Sensing 24 (5): 699–708. doi:10.1109/TGRS.1986.289617.

Lhermitte S, Verbesselt J, Verstraeten W, Veraverbeke S, and Coppin P. 2011 “Assessing Intra-annual Vegetation Regrowth after Fire Using the Pixel-based Regeneration Index.” ISPRS Journal of Photogrammetry and Remote Sensing 66 (1): 17–27. doi:10.1016/j.isprsjprs.2010.08.004.

Liu W, and Yamazaki F. 2012 “Object-based Shadow Extraction and Correction of High-resolution Optical Satellite Images.” IEEE Journal of Selected Topics in Applied Earth Observations and Remote Sensing 5 (4): 1296–1302. doi:10.1109/JSTARS.2012.2189558.

Masek JG, Vermote EF, Saleous NE, Wolfe R, Hall FG, Huemmrich KF, Gao F, Kutler J, and Lim TK. 2006 “A Landsat Surface Reflectance Dataset for North America, 1990–2000.” IEEE Geoscience and Remote Sensing Letters 3(1): 68–72. doi:10.1109/LGRS.2005.857030.

Masek JG, Goward SN, Kennedy RE, Cohen WB, Moisen GG, Schleeweis K, and Huang C. 2013 “United States Forest Disturbance Trends Observed Using Landsat Time Series.” Ecosystems 16 (6): 1087–1104. doi:10.1007/s10021-013-9669-9.

Meng R, Dennison P, D’Antonio C, and Moritz M. 2014 “Remote Sensing Analysis of Vegetation Recovery following Short-Interval Fires in Southern California Shrublands.” PloS One 9 (10): e110637. doi:10.1371/journal.pone.0110637. [PubMed: 25337785]

Miller JD, and Thode AE. 2007 “Quantifying Burn Severity in a Heterogeneous Landscape with a Relative Version of the Delta Normalized Burn Ratio (Dnbr).” Remote Sensing of Environment 109 (1): 66–80. doi:10.1016/j.rse.2006.12.006.

Montandon LM, and Small EE. 2008 “The Impact of Soil Reflectance on the Quantification of the Green Vegetation Fraction from NDVI.” Remote Sensing of Environment 112 (4): 1835–1845. doi:10.1016/j.rse.2007.09.007.

Pase CP, and Lindenmuth AW. 1971 “Effects of Prescribed Fire on Vegetation and Sediment in Oak-mountain Mahogany Chaparral.” Journal of Forestry 69 (11): 800–805.

Peterson SH, and Stow DA. 2003 “Using Multiple Image Endmember Spectral Mixture Analysis to Study Chaparral Regrowth in Southern California.” International Journal of Remote Sensing 24 (22): 4481–4504. doi:10.1080/0143116031000082415.

Pratt RB, Jacobsen AL, Ramirez AR, Helms AM, Traugh CA, Tobin MF, Heffner MS, and Davis SD. 2014 “Mortality of Resprouting Chaparral Shrubs after a Fire and during a Record Drought: Physiological Mechanisms and Demographic Consequences.” Global Change Biology 20 (3): 893–907. doi:10.1111/gcb.2014.20.issue-3. [PubMed: 24375846]

Roberts DA, Smith MO, and Adams JB. 1993 “Green Vegetation, Nonphotosynthetic Vegetation, and Soils in AVIRIS Data.” Remote Sensing of Environment 44 (2–3): 255–269. doi:10.1016/0034-4257(93)90020-X.

Röder A, Hill J, Duguy B, Alloza JA, and Vallejo R. 2008 “‘Using Long Time Series of Landsat Data to Monitor Fire Events and Post-fire Dynamics and Identify Driving Factors.’ A Case Study in the Ayora Region (Eastern Spain).” Remote Sensing of Environment 112 (1): 259–273. doi:10.1016/j.rse.2007.05.001.

Rouse J, Haas RH, Schell JA, and Deering DW. 1974 “Monitoring Vegetation Systems in the Great Plains with ERTS.” NASA Special Publication 351: 309–317.

Sawyer JO, Keeler-Wolf T, and Evens JM. 1995 A Manual of California Vegetation. Sacramento, California: California Native Plant Society.

Schoenherr AA 1992 A Natural History of California. Berkeley, California: University of California Press.

Shoshany M 2000 "Satellite Remote Sensing of Natural Mediterranean Vegetation: A Review within an Ecological Context." Progress in Physical Geography 24 (2): 153–178. doi: 10.1177/030913330002400201.

Song C, and Woodcock CE. 2003 "Monitoring Forest Succession with Multitemporal Landsat Images: Factors of Uncertainty." IEEE Transactions on Geoscience and Remote Sensing 41 (11): 2557–2567. doi:10.1109/TGRS.2003.818367.

Storey EA, Stow DA, and O'Leary JF. 2016 "Assessing Postfire Recovery of Chamise Chaparral Using Multi-temporal Spectral Vegetation Index Trajectories Derived from Landsat Imagery." Remote Sensing of Environment 183: 53–64. doi:10.1016/j.rse.2016.05.018.

Stow DA 1995 "Monitoring Ecosystem Response to Global Change: Multitemporal Remote Sensing Analyses" In Global Change and Mediterranean-Type Ecosystems, edited by Moreno JM and Oechel WC, 254–286. New York: Springer.

Syphard AD, and Keeley JE. 2017 "Historical Reconstructions of California Wildfires Vary by Data Source." International Journal of Wildland Fire 25 (12): 1221–1227. doi:10.1071/WF16050.

Syphard AD, Radeloff VC, Keeley JE, Hawbaker TJ, Clayton MK, Stewart SI, and Hammer RB. 2007 "Human Influence on California Fire Regimes." Ecological Applications 17 (5): 1388–1402. doi: 10.1890/06-1128.1. [PubMed: 17708216]

Todd SW, and Hoffer RM. 1998 "Responses of Spectral Indices to Variations in Vegetation Cover and Soil Background." Photogrammetric Engineering and Remote Sensing 64 (9): 915–921.

Turner MG 2010 "Disturbance and Landscape Dynamics in a Changing World." Ecology 91 (10): 2833–2849. doi:10.1890/10-0097.1. [PubMed: 21058545]

Venturas MD, MacKinnon ED, Dario HL, Jacobsen AL, Pratt RB, and Davis SD. 2016 "Chaparral Shrub Hydraulic Traits, Size, and Life History Types Relate to Species Mortality during California's Historic Drought of 2014." PloS One 11 (7): e0159145. doi:10.1371/journal.pone.0159145. [PubMed: 27391489]

Veraverbeke S, Lhermitte S, Verstraeten W, and Goossens R. 2010 "The Temporal Dimension of Differenced Normalized Burn Ratio (Dnbr) Fire/burn Severity Studies: The Case of the Large 2007 Peloponnese Wildfires in Greece." Remote Sensing of Environment 114 (11): 2548–2563. doi:10.1016/j.rse.2010.05.029.

Vermote E, Justice C, Claverie M, and Franch B. 2016 "Preliminary Analysis of the Performance of the Landsat 8/OLI Land Surface Reflectance Product." Remote Sensing of Environment 185: 46–56. doi:10.1016/j.rse.2016.04.008. [PubMed: 32020955]

Vila JPS, and Barbosa P. 2010 "Post-fire Vegetation Regrowth Detection in the Deiva Marina Region (Liguria-italy) Using Landsat TM and ETM+ Data." Ecological Modelling 221 (1): 75–84. doi: 10.1016/j.ecolmodel.2009.03.011.

Wing MG, Burnett JD, and Sessions J. 2014 "Remote Sensing and Unmanned Aerial System Technology for Monitoring and Quantifying Forest Fire Impacts." International Journal of Remote Sensing Applications 4 (1): 18–35. doi:10.14355/ijrsa.2014.0401.02.

Xiao J, and Moody A. 2005 "A Comparison of Methods for Estimating Fractional Green Vegetation Cover within A Desert-to-upland Transition Zone in Central New Mexico, USA." Remote Sensing of Environment 98 (2–3): 237–250. doi:10.1016/j.rse.2005.07.011.

Yang X, and Guo X. 2014 "Quantifying Responses of Spectral Vegetation Indices to Dead Materials in Mixed Grasslands." Remote Sensing 6 (5): 4289–4304. doi:10.3390/rs6054289.

Zedler PH, Gautier CR, and McMaster GS. 1983 "Vegetation Change in Response to Extreme Events: The Effect of a Short Interval between Fires in California Chaparral and Coastal Scrub." Ecology 64 (4): 809–818. doi:10.2307/1937204.

Zhu Z, and Woodcock CE. 2012 "Object-based Cloud and Cloud Shadow Detection in Landsat Imagery." Remote Sensing of Environment 118: 83–94. doi:10.1016/j.rse.2011.10.028.

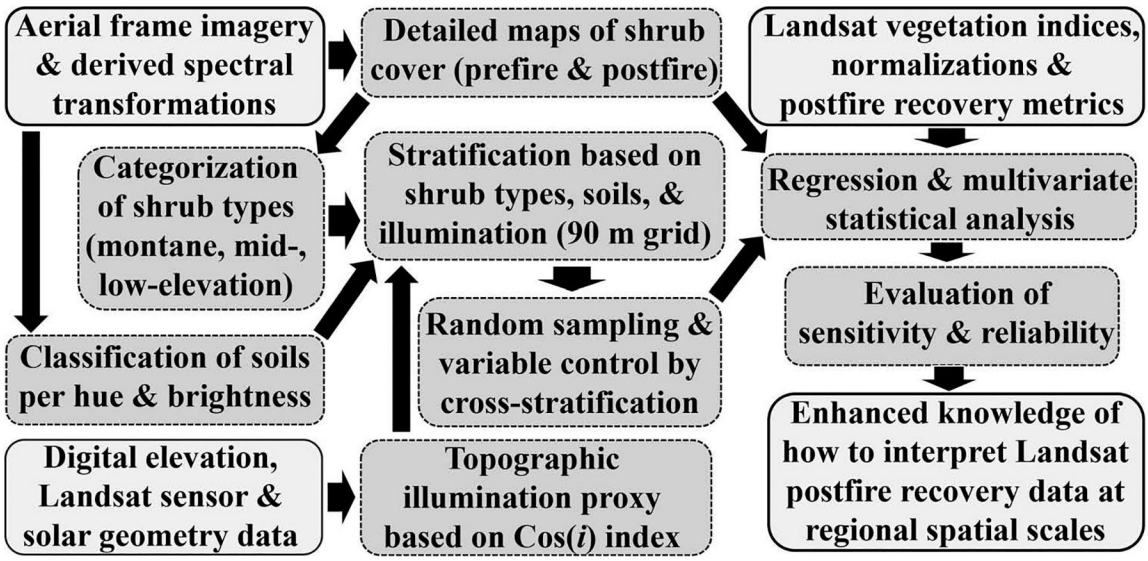

Figure 1.

Analytical workflow used to evaluate Landsat-based postfire recovery assessments with respect to potential uncertainties due to landscape heterogeneity.

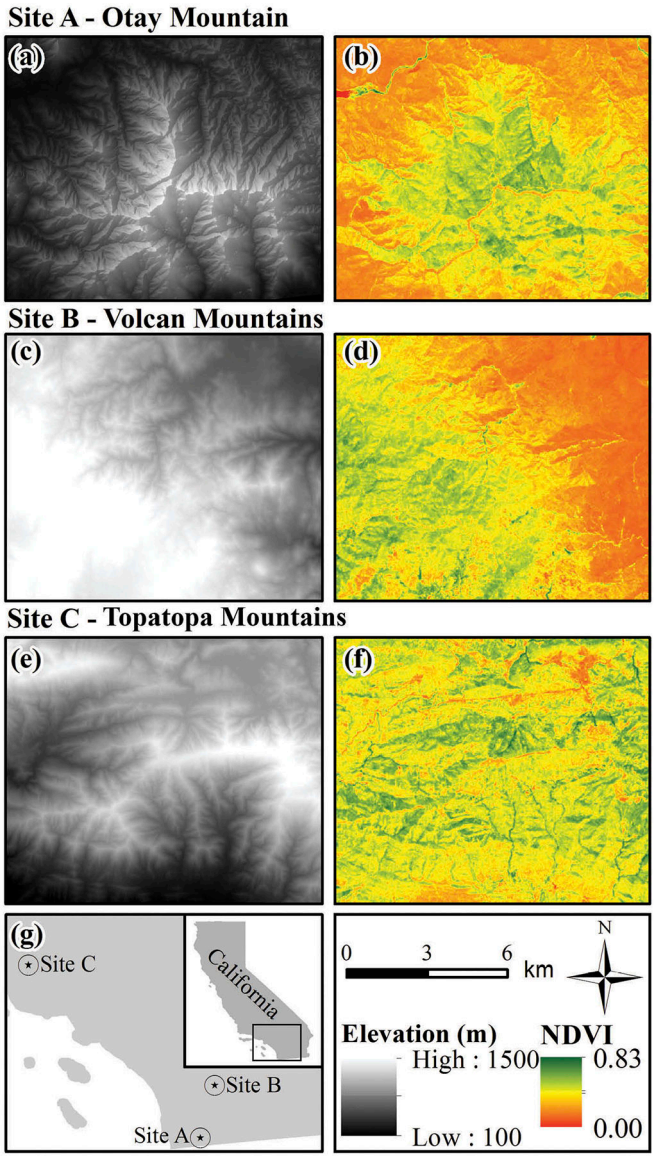

Figure 2.

Study area elevation (left) and vegetation patterns represented by NDVI (right) derived from Landsat 5 images of summers 1989–1991. Map scale and display contrast are consistent among figure panes. Study areas extend slightly view in Site B and Site C.

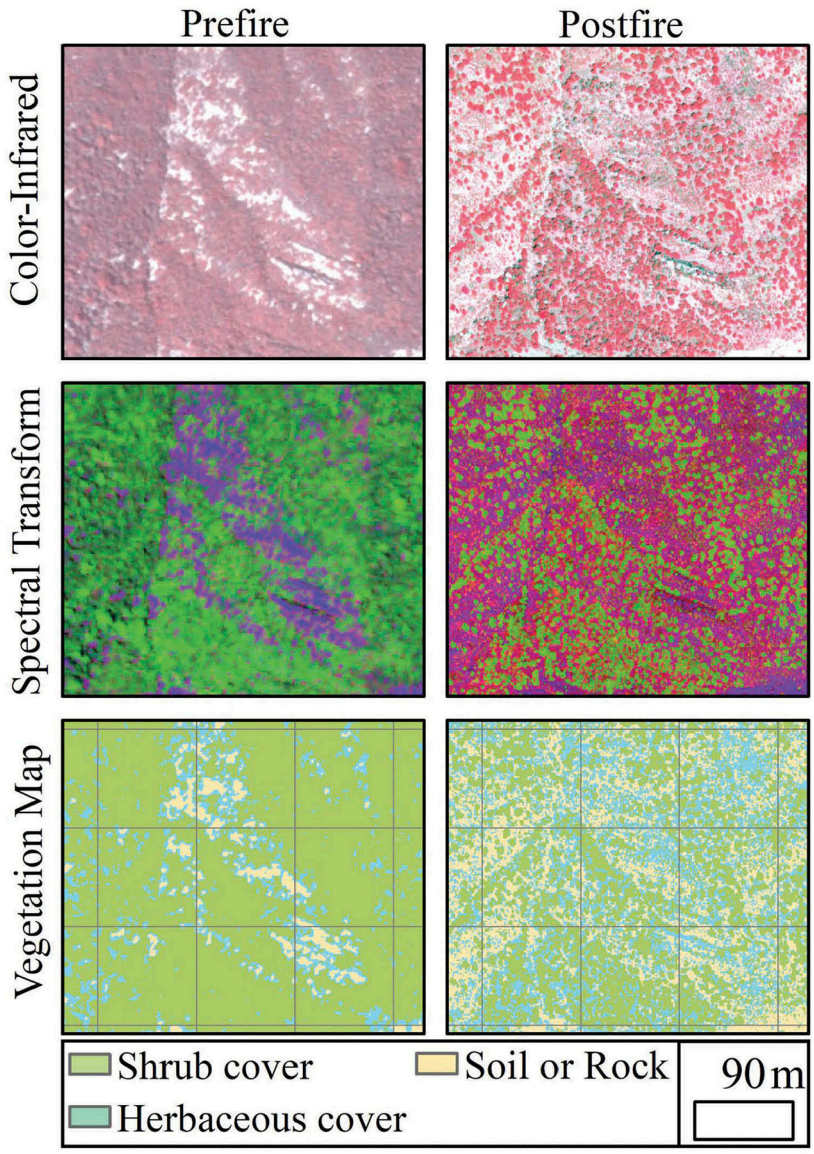

Figure 3.

Illustration of source images and shrub cover maps used to validate postfire recovery variations. Fractional cover values were aggregated in 90-X-90 m grid elements aligned to 3-X-3 Landsat pixel blocks. Spectral transforms based on ortho-images are shown as false-color composites (green = NDVI, blue = average of red and green bands, red = red/green band ratio), which were classified to derive the shrub cover maps.

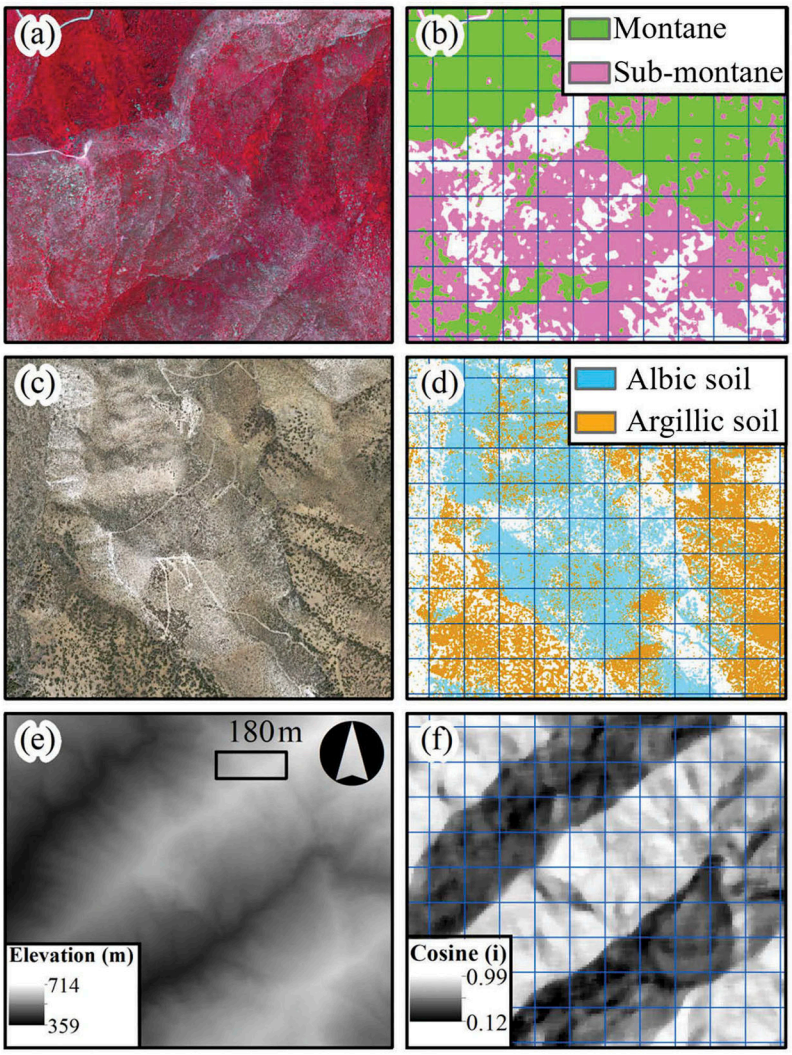

Figure 4.

An illustration of how land cover (soils and vegetation) and terrain (illumination) data were tabulated to vector grids as percent composition. Map frames show shrub types (*a* and *b*), soil types (*c* and *d*), and cosine of solar incidence angle (*f*) on 21 June (based on a 10 m digital elevation model (*e*)). Unclassified areas are shown in white. Tabulations of the land cover and illumination (subsequently classified) were based on 90-x-90 m grids.

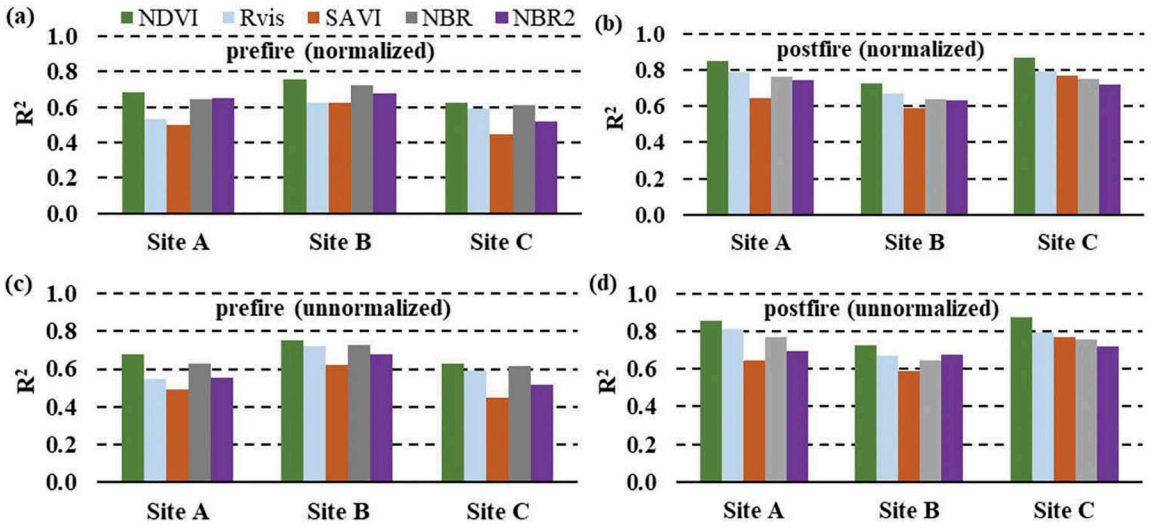

Figure 5.

R^2 values based on ordinary least-squares functions used to correlate trajectory-based Landsat SVI values to total shrub cover in study sites A, B, and C (estimated from ortho-imagery). Prefire SVI values are based on five-year means; postfire values are derived from best-fit trajectories at the year 2016. Results derived with (parts *a* and *b*) and without (parts *c* and *d*) phenological normalization of Landsat data are provided.

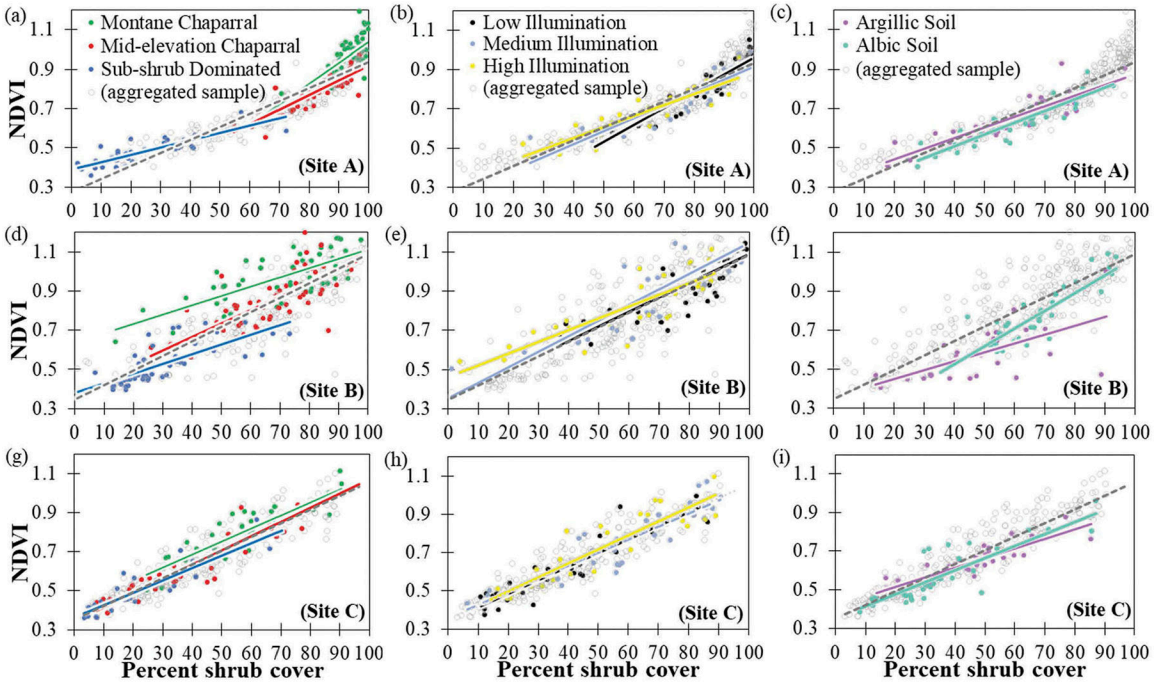

Figure 6.

Scatter plots depicting empirical relations of fractional shrub cover to Landsat NDVI trajectories (at the year 2016) organized according to analytical strata of shrub type (*a*, *d*, and *g*), soil type (*c*, *f*, and *i*), and terrain illumination level (*b*, *e*, and *h*). Stratum-specific data are colored and overlaid on aggregated data (all points) from Site A (n =369), Site B (n =378), and Site C (n =326). Best-fit lines are color-coordinated; dashed gray lines represent aggregate-level trends. All samples are based on 90 m grids.

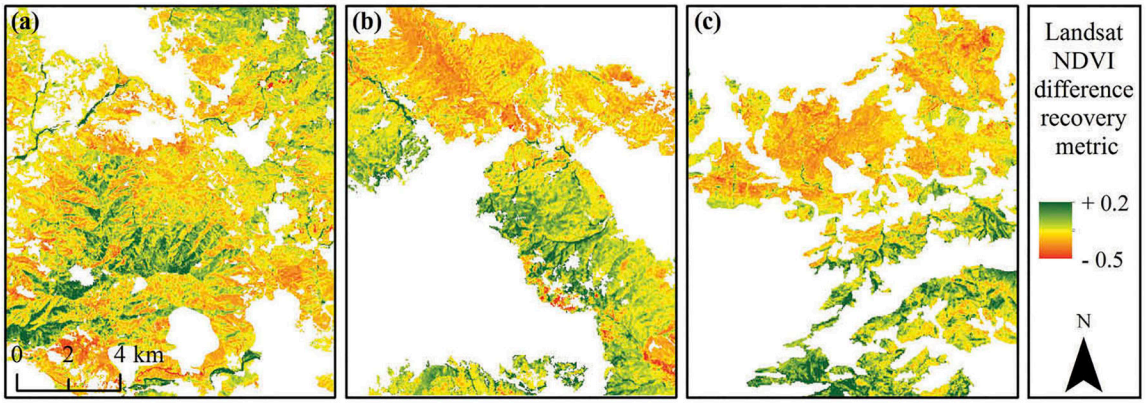

Figure 7.

Illustration of heterogenous patterns of postfire recovery in the three study areas, derived from Landsat NDVI difference metric applied to temporal trajectories, based on surface reflectance images of unaltered (30 m) spatial resolution.

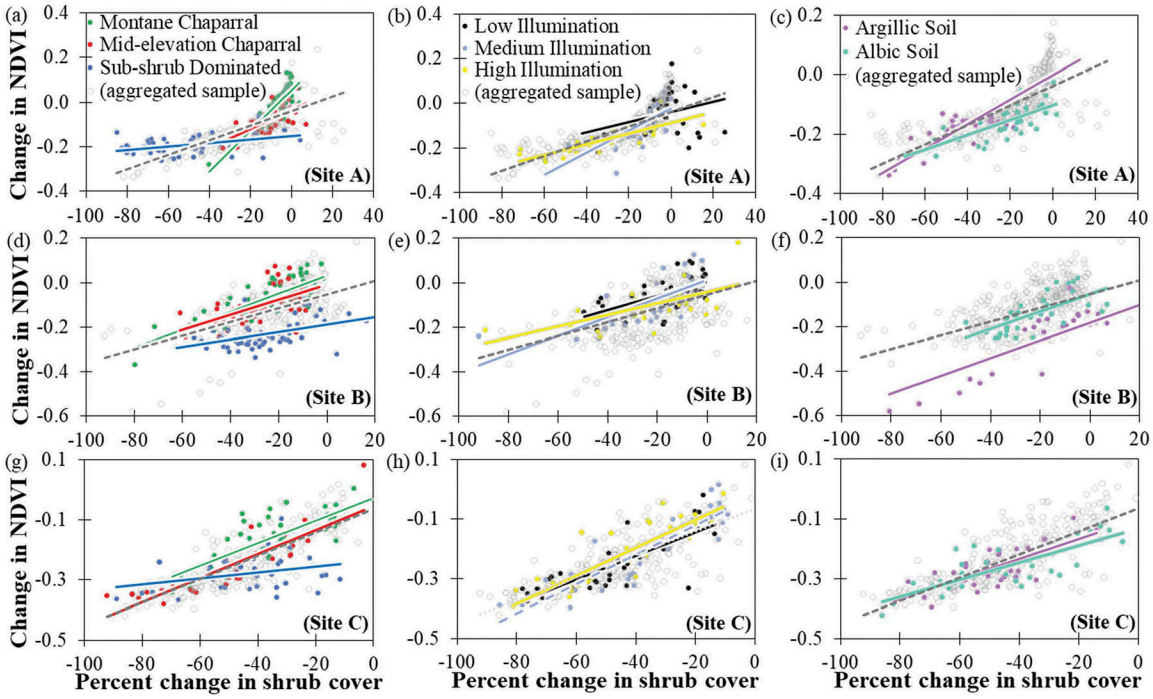

Figure 8.

Scatter plots relating shrub cover (absolute) percent change *versus* postfire recovery (difference) metrics derived from Landsat NDVI trajectories. Data points are colored according to analytical strata of shrub type (*a*, *d*, and *g*), soil type (*c*, *f*, and *i*), and terrain illumination level (*b*, *e*, and *h*). Stratum-specific data are colored and overlaid on aggregated data (all points) from Site A (n =369), Site B (n =378) and Site C (n =326). Best-fit lines are color-coordinated; dashed gray lines represent aggregate-level trends. All samples are based on mean values of 90 m grid units.

Table 1.

Factor *p*-values from multi-variate linear regressions of stratum membership, fractional shrub cover, Landsat NDVI trajectory values in the year 2016 ($\alpha = 0.05$). Significant values are in bold font.

Stratum	Site A	Site B	Site C
Sub-shrub Dominated	0.784	0.477	**0.015**
Sub-montane Chaparral	0.085	**0.049**	0.076
Montane Chaparral	**< 0.001**	**< 0.001**	0.989
Low Illumination	0.675	**0.024**	**0.020**
Medium Illumination	0.283	**0.008**	0.056
High Illumination	0.327	**0.015**	0.138
Argillic Soil	0.271	**< 0.01**	**< 0.01**
Indistinct Soil	0.128	**0.045**	0.141
Albic Soil	**< 0.01**	0.778	**< 0.01**

Table 2.

R^2 values stemming from univariate linear regressions of change in fractional shrub cover *versus* postfire recovery metrics derived from Landsat NDVI.

Normalized	Site A	Site B	Site C	Mean
Difference metric	0.54	0.26	0.53	0.44
Scaled recovery metric	0.05	0.05	0.43	0.18
Ratio metric	0.51	0.29	0.59	0.46
Unnormalized				
Difference metric	0.55	0.27	0.58	0.47
Scaled recovery metric	0.01	0.00	0.43	0.15
Ratio metric	0.53	0.30	0.59	0.47

Table 3.

Factor *p*-values stemming from multi-variate linear regressions of stratum membership, change in fractional shrub cover, and trajectory difference postfire recovery metrics based on Landsat NDVI ($\alpha = 0.05$). Significant values are in bold font.

Stratum	Site A	Site B	Site C
Sub-shrub Dominated	0.896	**0.004**	< **0.001**
Sub-montane Chaparral	0.839	**0.003**	0.111
Montane Chaparral	< **0.01**	< **0.001**	0.973
Low-illumination	0.581	< **0.001**	**0.029**
Medium-illumination	0.835	< **0.01**	0.169
High-illumination	0.357	**0.019**	0.272
Argillic Soil	0.898	< **0.001**	**0.021**
Indistinct Soil	0.359	**0.013**	0.114
Albic Soil	0.637	0.561	< **0.01**